A Beginner's Guide to Space Weather and GPS
Updated February 21, 2008
Professor Paul M. Kintner, Jr.

with acknowledgements to

M. Psiaki, T. Humphreys, A. Cerruti, B. Ledvina, A. Mannucci, D. Gary, E. de Paula, and L. Shelton

I. Introduction

This brief paper is written for GPS engineers or systems designers who need to know about space weather. Just as an architect might need to know about hurricanes or tornadoes, characterizing space weather enables designers to understand vulnerabilities in their designs, to create more robust designs, and to determine how best to avoid risk. Space weather is a somewhat arcane topic studied by a few space scientists who, by and large, lack a working knowledge of GPS signals and receivers. On the other hand, GPS and GNSS comprise a growth industry limited only by the imagination and are populated by engineers with little knowledge of space weather. Cornell University's faculty are award-winning experts in both space weather and GPS receiver design and have an international reputation for their work at the intersection of space weather and GPS. These perspectives motivated the creation of this beginner's guide.

The objective is to advise the practicing engineer of when and how GPS systems may be affected by space weather. The high-level description below is adequate for determining whether further investigation is required. For those wanting to probe the subject more deeply, the bibliography at gps.ece.cornell.edu is recommended.

The paper's organization consists of an overview of space weather, how the ionosphere affects GPS signals, a description of ionospheric climate and weather, and strategies for mitigating the effects of space weather.

II. Overview of Space Weather

Space weather, with one important exception, begins at the sun. The sun exhibits an 11-year cycle of sunspots that are visible manifestations of increased solar magnetic field. The last sunspot maximum was in 2000 and the next one is expected in 2011. The maxima are somewhat broad and, for the purpose of space weather, last 3-5 years. During the sunspot maximum, the solar magnetic field is destroyed in solar flares, giving up its energy in solar ultraviolet (uV) light, x-rays, energetic particles (MeV protons), coronal mass ejections (CMEs), and a "stormy" solar wind. Certain larger flares produce solar radio bursts of broadband noise from 10 MHz to 10 GHz that may directly affect GPS receivers on the dayside of the earth. Although larger solar flares produce solar radio bursts, a one-to-one relation between the size of a solar flare and the intensity of a solar radio burst does not exist.

Coronal mass ejections and stormy solar winds frequently reach the earth if they originate on the part of the sun facing the earth. These ejections arrive as supersonic shock waves, frequently carrying high energy particles. Because the solar wind is fully ionized, it first encounters the earth's magnetic field. The high energy particles can directly reach the upper atmosphere over

the north and south poles, endangering transpolar air flights. Depending on how the solar magnetic field captured in the solar wind encounters the earth's magnetic field, a magnetic storm may develop. In a magnetic storm the Van Allen radiation belts surrounding the earth are rearranged, creating a "doughnut" of 100 keV plasma around the earth at 3-4 Re that carries a ring current. This current creates a magnetic field opposite to the earth's magnetic field at the surface of the earth. The disturbance magnetic field may amount to 1% or more of the earth's field and thus is called a magnetic storm. The radiation belts pose a hazard to MEO and GEO spacecraft because of spacecraft charging in the short run and solar cell degradation in the long run, and are also potentially fatal to astronauts. During these storms the rearrangement of the earth's magnetic field and creation of the ring current drive disturbances in the ionosphere as well (see section IV).

An important aspect of the solar cycle is that the average solar uV increases substantially at solar maximum. Since solar uV produces the ionosphere by direct ionization and heats the thermosphere, the ionosphere is denser and thicker during solar maximum. Hence GPS signals are more strongly affected by the ionosphere during solar maximum.

Space weather affecting GPS can be roughly organized into four categories. At equatorial or tropical latitudes the ionosphere frequently will affect GPS signals with the severity modulated by the solar uV intensity, as noted above. However, the occurrence of ionospheric weather in the tropics is usually suppressed by solar and magnetic storms. At mid-latitudes, ionospheric weather is dominated by magnetic storms. Large storms move the aurora equatorward over the United States, and all magnetic storms have the potential to move equatorial plasma poleward and create thicker ionospheres with sharp gradients. At high latitudes, the northern lights, and ionospheric structures called "blobs" occur frequently but usually do not have a major impact on GPS signals. Finally, GPS receiver operation can be affected directly by solar radio bursts that increase the natural noise levels at 1.2 GHz and 1.6 GHz.

III. Ionospheric Effects on GPS signals

The ionosphere is composed of plasma that alters transiting radio waves in three ways. First, the wave group velocity decreases as

$$\mathrm{v}_\mathrm{g} = c\sqrt{1-\omega_{pe}^2/\omega^2}$$

where

$$\omega_{pe} = \sqrt{n_e q^2/\varepsilon m_e}$$

is called the plasma frequency with a value of typically 1-10 MHz (6.28-62.8 rad/s). A decreased group velocity yields a code delay. Second, the phase velocity increases as

$$\mathrm{v}_\phi = \frac{c}{\sqrt{1-\omega_{pe}^2/\omega^2}},$$

which yields a phase advance. Third, plasma density irregularities having scale lengths equivalent to the Fresnel length scatter radio signals, which then add constructively and destructively at the receiver. The Fresnel length is $\sqrt{2\lambda d}$ where λ is 19 cm for the L1 signal and d is about 350 km for a 90° elevation satellite. For GPS signals the Fresnel length is about 350 m or longer. Figure 1 illustrates these three processes.

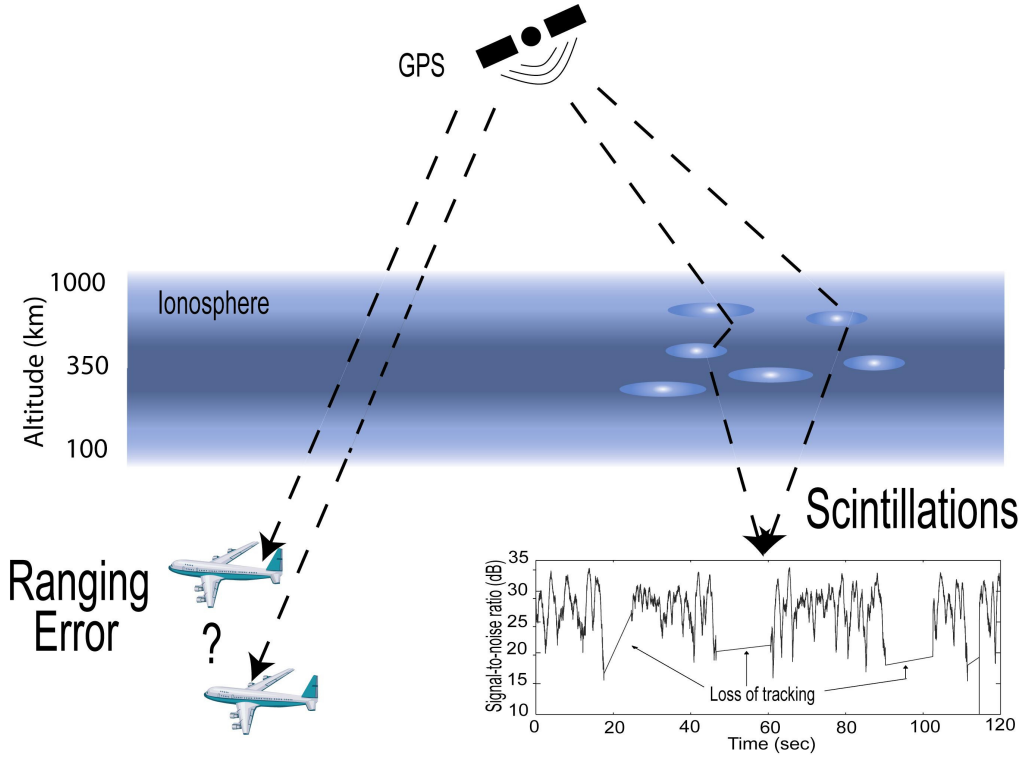

Figure 1. Cartoon of ionospheric effects on GPS signals. Both code and phase ranging errors are created by signal propagation throughout the ionosphere. If ionospheric density irregularities exist, the signals are scattered, producing amplitude scintillations.

Since the only variable parameter in the group or phase velocity is the ionospheric electron density (n_e), the amount of group delay or phase advance is given by the integrated electron density along the signal path, called the total electron content (TEC), as

$$\delta t = \frac{q^2}{2c\varepsilon m_e f^2 (2\pi)^2} \int_\rho n_e d\rho$$

where the integral represents TEC. In mks units this reduces to:

$$\delta t = \frac{40.3}{cf^2} \times TEC\,.$$

TEC is the number of electrons in a volume with a one-meter-square cross section and length equal to the signal path. TEC is typically expressed in TEC units, and one TECU=10^{16}

electrons/m^2. One TECU produces about 16 cm of code delay or range error. Since the electron density is much larger in the ionosphere than any other portion of the signal path, the ionospheric plasma contributes the majority of the TEC integral.

Scintillations are produced by signals scattered in the ionosphere that add in a phase-wise sense at the receiving antenna. Amplitude scintillations are characterized by both amplitude increases (constructive interference) and amplitude decreases (destructive interference). Phase scintillations are produced both by changes in TEC and through interference. The relative contributions are still a matter of research. The Fresnel length can be derived by thinking of ionospheric scattering as being equivalent to a two-slit diffraction pattern. The Fresnel length, then, is a two-slit separation that yields a single wavelength phase shift at the receiver. Scintillations should be thought of as a pattern moving across the ground that yields temporal behavior at a receiver. As an analogy, ionospheric irregularities are like a "picket fence" moving across the sky, interrupting the GPS signal and producing a time-varying signal amplitude. The time scale, then, is given by the Fresnel length divided by the ionospheric velocity. This velocity is quite variable, but a typical value is 100 m/s, yielding a time scale of a few seconds. The time scale is complicated by the fact that the GPS signal path is also moving laterally in the ionosphere. In some cases the GPS signal lateral velocity can match the ionospheric lateral velocity, yielding longer time scales.

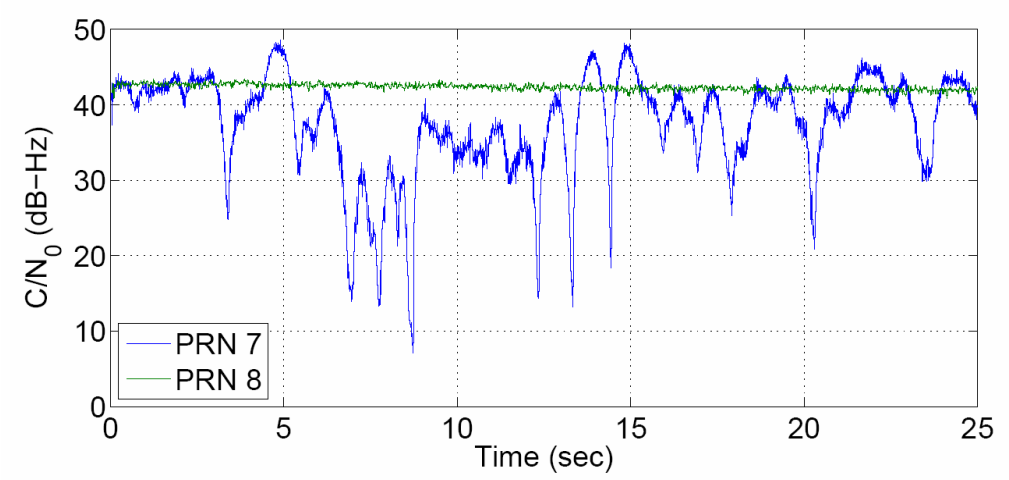

Figure 2. The carrier-to-noise ratios (signal strength) of two GPS satellite signals, one of which is scintillating while the other is not. (Figure courtesy of T. Humphreys.)

The amplitude of destructive interference can be large. Figure 2 shows two GPS signals being tracked simultaneously during a period when one of the two signals, PRN 8, is not scintillating. The other signal, PRN 7, is exhibiting fades (destructive interference) of up to 40 dB. This example was produced with a digital storage receiver in which the GPS bandwidth is captured at 5.7 Msamples/s, stored in mass memory, and then processed later with a MATLAB software receiver. The scintillating signal is tracked with a Kalman filter tracking loop and a variable bandwidth filter. Hardware receivers normally cannot track in this environment because they typically fail at signal strengths of 27-28 dB.

GPS receivers track not only the coarse acquisition code but also the signal phase or frequency. Phase lock loops are particularly vulnerable during deep fades because a deep fade is

associated with a sudden half-cycle phase jump. Figure 3 shows examples of deep fades with which are associated half-cycle phase jumps. This signal has been tracked to very low levels of C/No by wiping off the data bits, narrowing the phase lock filter, and tracking both forward and backward in time. In addition we have chosen a time when the scintillation time scales are particularly slow. At 98 s a clear example of a deep fade and a half-cycle phase jump exists, with several less extreme examples present in the figure. The phase jump can be either positive or negative with equal probability. The reason for the phase jump is apparent if one thinks of two phasors, one representing the direct signal and one representing the interfering diffracted signal. The resulting amplitude is determined by attaching the tail of the diffracted signal phasor to the head of the direct signal phasor. Very deep fades occur when the diffracted signal phasor sweeps near the origin, producing very small resultants and half-cycle phase flips as it crosses near the origin. At Cornell University we call the combination of a deep fade and a half-cycle phase jump a "canonical fade".

Examining the time history of GPS signal amplitude fades is not efficient for representing scintillation climate and weather. Instead, two indices are used to describe the morphology of ionospheric scintillations. The first is called the S4 index, the ratio of the standard deviation of the signal power fluctuations over the average ionospheric power. This S4 index is typically calculated over a period of one minute, although there is no standard. The second is called sigma-phi and is the standard deviation of the phase fluctuations. For example, the S4 index of PRN 7 in Figure 2 exceeds 1.

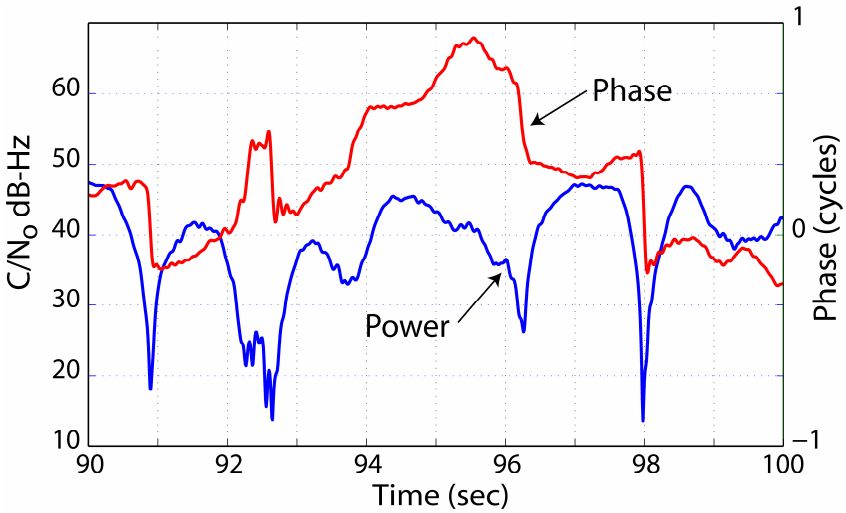

Figure 3. Example of deep fades accompanied by half-cycle phase jumps in the L1 GPS signal. (Figure courtesy of T. Humphreys.)

IV. Ionospheric Climate and Weather

A. The Equatorial Ionosphere

The equatorial ionosphere is organized around the geomagnetic equator, which differs substantially from the geographic equator. Figure 4 shows an assimilative model of global ionospheric vertical TEC for solar noon at about 110° west longitude during solar minimum.

The model assimilates GPS TEC data from receivers (shown as black dots) and combines them with a model based on physics equations to yield a global TEC map.

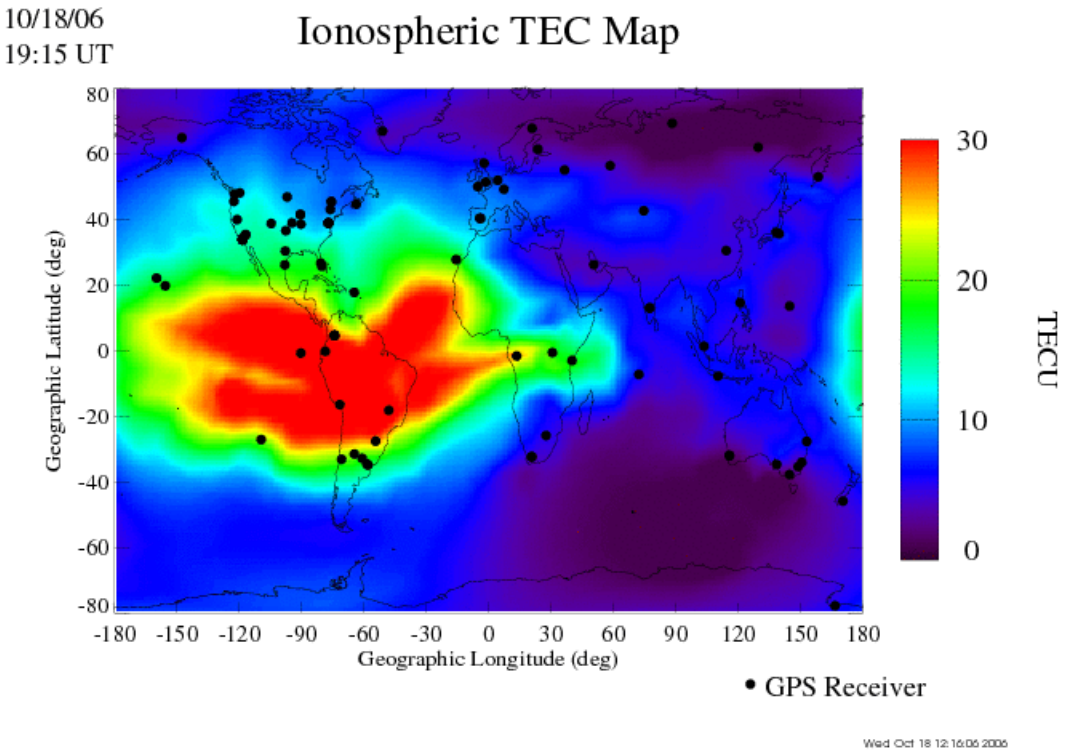

Figure 4. Global map of TEC. (Figure courtesy of NASA/JPL.)

Figure 4 illustrates several features of the equatorial ionosphere. The peak TEC values occur during the afternoon, as the peak TEC organizes into two bands at about 15° on either side of the geomagnetic equator. These bands are referred to as the Appleton or equatorial anomalies. During the day, solar heating of the thermosphere carries the ionosphere upward. At the equator the magnetic field is horizontal and then tilts downward for more poleward latitudes. The rising ionospheric plasma at the equator falls down magnetic field lines to higher latitudes, creating the anomalies. Since the anomalies typically (but not always) host the largest ionospheric electron densities, this is where GPS signals are usually the most disturbed.

After sunset the horizontal magnetic field at the equator holds the ionospheric plasma up, allowing an electromagnetic equivalent of the Rayleigh-Taylor instability to be genrated (upside down water glass). If conditions are favorable, within an hour after sunset, bubbles form in the ionospheric plasma, rising upwards a few hundred to a thousand km. The bubbles are extended along the magnetic field lines and, as they rise upwards, the projections of the field lines move to higher latitudes, eventually reaching the anomalies. The upward movement of the bubble evolves over about one hour, creating electron density gradients and ionospheric irregularities. After the instability has spent its course, the gradients and irregularities remain embedded in the ionosphere for the reminder of the night, slowly dissipating. At sunrise the ionosphere refills and fills in what remains of the bubble and the ionospheric irregularities.

Figure 5 shows an example of an equatorial ionospheric bubble. On the left-hand side is an elevation-azimuth plot of PRN 14. The signal power and TEC are shown on the right. In the lower right is the TEC record. At lower elevations the oblique slant factor through the ionosphere creates larger TEC values. The satellite signal encounters a bubble between 2200 and 2400 LT where the TEC values are structured and depressed. After the signal exits the bubble, the TEC again increases as the elevation decreases. The GPS signal amplitude shown in

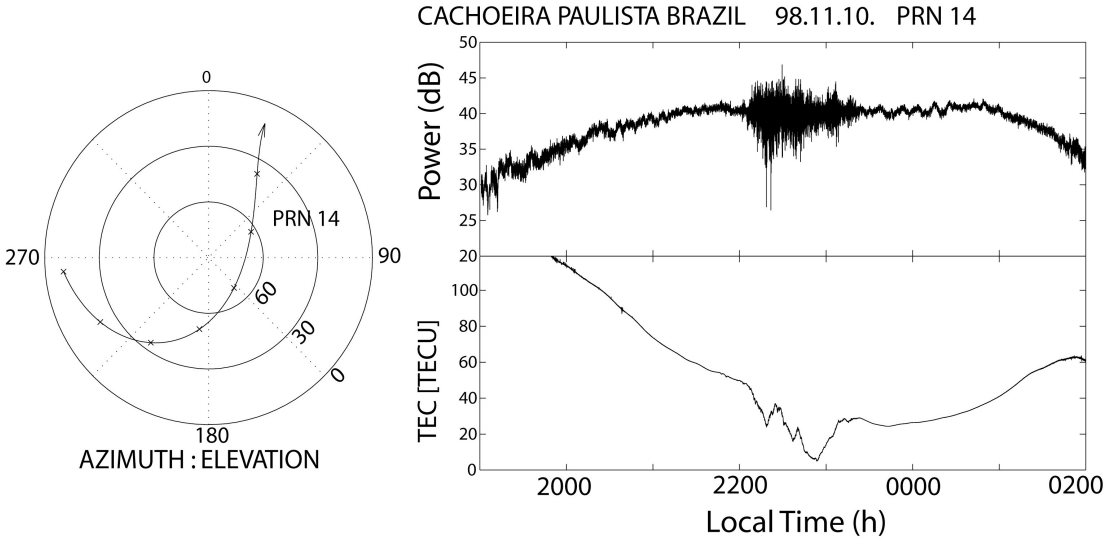

Figure 5. Example of an equatorial plasma bubble and amplitude scintillations.

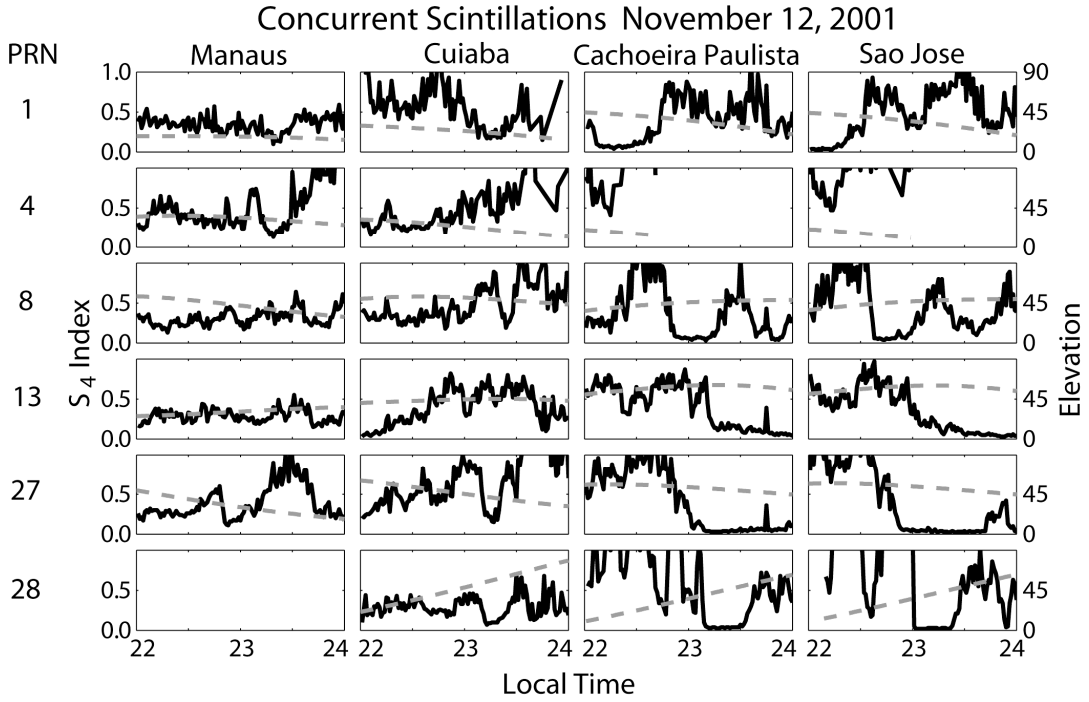

Figure 6. S4 values for four sites and six GPS satellites during a two-hour period. The elevation of each satellite is plotted as a dashed line.

the upper right-hand panel initially increases as the satellite rises in elevation. The change in amplitude results from the antenna gain pattern, which is generally lower at lower elevations. At the time the signal encounters the bubble, it also begins to scintillate in amplitude, which ends when the signal exits the bubble. That the signal amplitude both increases and decreases is a key feature of scintillations. This is a moderate event about three years before the last solar maximum.

Scintillations can be much more extensive. Figure 6 shows an example of the S4 value (defined above) at four locations spread across Brazil for six satellites seen in common by all of the receivers. Essentially all of the satellites are scintillating at all of the locations for the two-hour period. Exceptions can be seen at Cachoeira Paulista and São José for PRN 28 between 2330 and 2330 LT. One should not assume that scintillations will only occupy a fraction of the sky for brief periods.

As explained above, bubbles and the scintillations associated with them begin shortly after sunset. Predicting the existence of scintillations on a specific night is not straightforward. From a climatological viewpoint, bubbles are more likely to occur when the foot points of a magnetic field line enter darkness simultaneously. So, for regions on the globe where lines of geographic longitude and lines of magnetic longitude are parallel, bubbles are more likely to occur during the equinoxes in September and March. Where the lines are not parallel, the period of maximum bubble occurrence is shifted. For example, in Brazil the season for bubbles is November through February.

The next factor to consider is geomagnetic activity. Magnetic storms tend to suppress the occurrence of bubbles before local midnight and enhance their occurrence after local midnight. During solar maximum and during the peak season, bubbles may occur on 70-80% of the nights. The ability to predict the occurrence of bubbles on a given night is an area of active research.

B. Mid-latitude Space Weather

At mid-latitudes we know less about ionospheric space weather than at high latitudes, where the ionosphere is frequently disturbed by the aurora, and at low or equatorial latitudes. The more active regions at high and low latitudes attract more attention from scientists. More attention means more resources are allocated to these regions, and the mid-latitudes are further neglected. A recent break with this tradition is the creation of the Cooperative Operating Receivers System (CORS) of GPS receivers in the United States. Although not established for investigating the ionosphere, the publicly available GPS and TEC data have enabled regional imaging of the mid-latitude ionosphere for the first time. These images reveal dramatic changes in the mid-latitude ionosphere during ionospheric storms. Large swaths of ionosphere, denser and thicker than anywhere else, form and sweep across the United States, heading poleward into the polar cap. These events occur during magnetic storms and host steep electron density gradients as well as irregularities, producing scintillations. Figure 7 shows an example of a mid-latitude ionospheric storm. In this case, TEC values from the reference receiver have been combined with an ionospheric assimilation model to display a dense finger of increased TEC extending across the eastern seaboard of the United States and northward to Hudson Bay.

Mid-latitude ionospheric storms occur during the first several hours of the onset of a magnetic storm. TEC values exceeding 200 TECU vertical have been recorded over the continental United States. Several dozen mid-latitude ionospheric storms have been observed

since they were first discovered in 2002. Understanding these storms is an active area of research, addressing such questions as, "Do they occur at other longitudes besides North America?" "Does the new ionospheric plasma come from the tropics or is it generated locally?" "Do mid-latitude ionospheric enhancements move poleward and into the polar cap?"

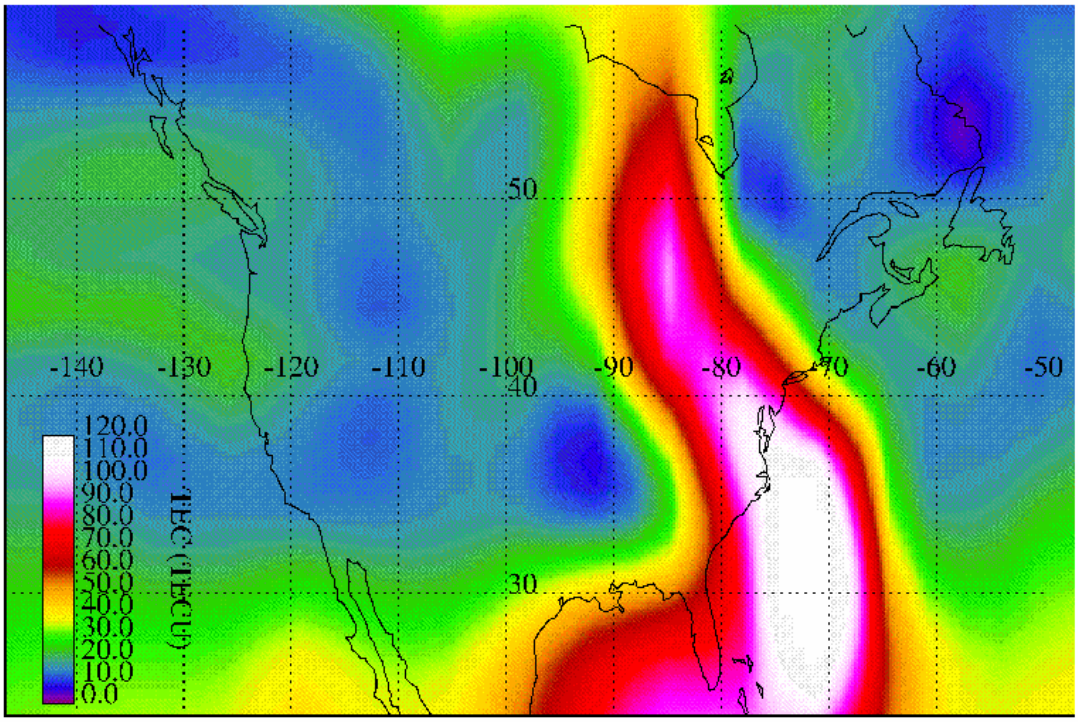

Figure 7. Example of TEC variations over the United States during a magnetic storm. (Figure courtesy of R. Schunk.)

The question of whether mid-latitude ionospheric storms produce scintillations has been only partially answered. Only two good observations of strong GPS signal scintillations at mid-latitudes exist. The first observation was made at Ithaca, NY and the second observation was made at Kyoto, Japan. Both observations were made during relatively minor magnetic storms, yet in both cases the receivers lost lock on the scintillating signals. Figure 8 shows the example of scintillations at Ithaca, NY. The upper panel shows a measure of the magnetic storm strength, called Dst, and larger negative values correspond to more intense storms. In this case the maximum negative value was -100 nT compared to -500 nT during the largest magnetic storms. The middle panel shows the received signal power (C/No) for a GPS satellite during the time shown in gray in the upper panel. Just after 2400 UT the signal began to scintillate dramatically and continued to do so until the satellite set near 2730 (0330) UT. The lower panel shows that TEC values before the scintillation began were about double their normal value. A large gradient in TEC near 2400 UT, accompanied by irregular structure, coincides with the most intense scintillations. The expanded received power plot in the lower right of Figure 1 comes from the period near 2410.

Figure 8 is the only example of scintillations observed at Ithaca during the last solar maximum. The fact that these scintillations were observed at all was serendipitous since the observations were obtained by a receiver during testing prior to shipment to Brazil. Continuous

GPS scintillation monitoring began a year later and, since that time, no further events have been observed. Another event at Kyoto, Japan on July 27, 2004 was reported in association with a similar magnetic storm, using the same GPS receiver design. Hence only two robust observations exist. As noted earlier, these observations may be infrequent because they are rare or because there are few GPS scintillation receivers to monitor their occurrence.

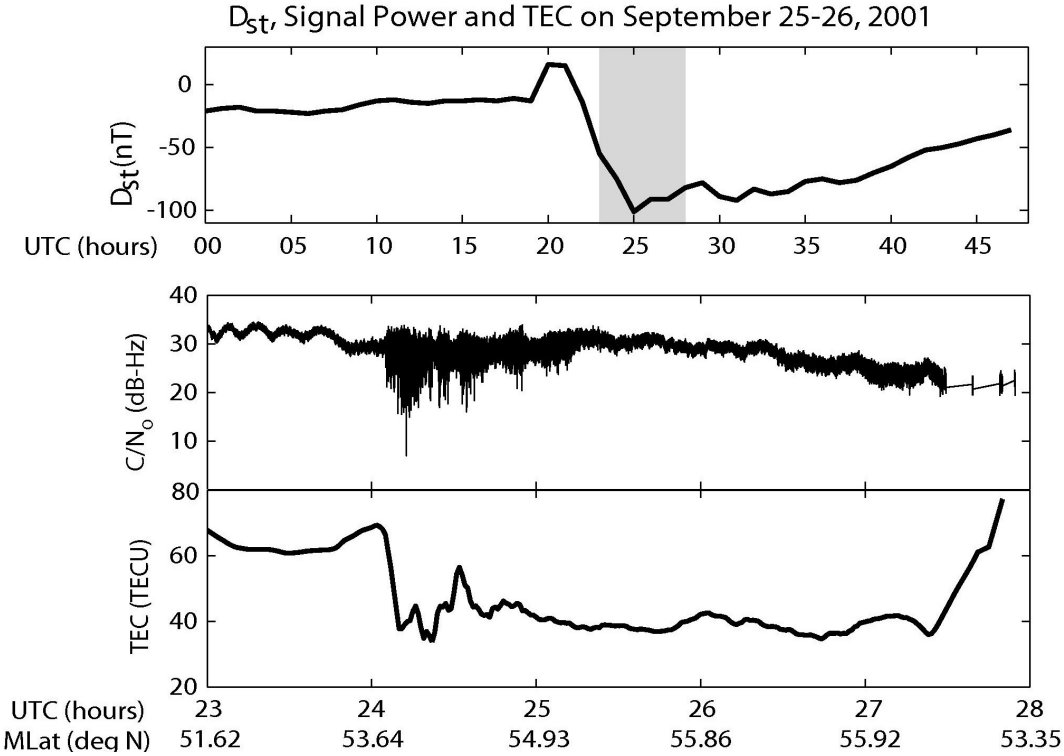

Figure 8. Example of GPS signal scintillations in the middle panel.

C. High Latitude Space Weather

High-latitude space weather is important primarily at VHF and UHF frequencies but not at the L-band frequencies used by GPS because ionospheric densities typically are smaller than those in the tropics or at mid-latitudes during magnetic storms. Smaller densities are less likely to affect higher frequency signals. There has been one report of GPS amplitude scintillations associated with an active auroral arc. Many reports also exist of auroral arcs causing cycle slips in GPS receiver phase lock loops. Density gradients affect systems such as WAAS but, with the exception of very intense aurora, GPS signals appear to be robust at high latitudes.

V. Solar Radio Burst Impacts on GPS

Solar radio bursts are produced during flares and are generally broadband, 0.1-10 GHz, radio emissions which may contain spectral signature. Until recently it was believed that solar radio bursts were not intense enough to affect GPS signals. On December 6, 2006 this belief was challenged by a solar radio burst that exceeded 1,000,000 SFU (1 SFU or one solar flux unit = 10^{-22} $Wm^{-2}Hz^{-1}$), more than ten times larger than any previous solar radio burst and nearly 100

time larger than any solar radio burst at solar minimum. Figure 9 shows the solar radio burst spectrum between 1 GHz and 2 GHz (top panel), along with the C/No at the Houston WAAS receiver (bottom panel). The solar radio burst began at about 1840 UT, continuing to about 1950 UT. In the bottom panel the blue line is the C/N0 for the day prior to the solar radio burst and the red line is the C/No for the day of the solar radio burst. C/No only decreases. There are no increases in C/No as there are for scintillations. The period of interference affecting the GPS receiver extends about 45 minutes and is impulsive with some signal reductions reaching roughly 18 dB. It should be emphasized that the WAAS receivers are very robust, using atomic clocks to reduce phase noise and small bandwidth phase lock loops to further reduce their noise contribution. Other examples exist of less robust, single-frequency receivers and many semi-codeless, dual-frequency receivers losing lock during this event. The solar radio burst appeared to impact all receivers on the sunlit disk of the earth, and for a single receiver it affected all GPS signals in view.

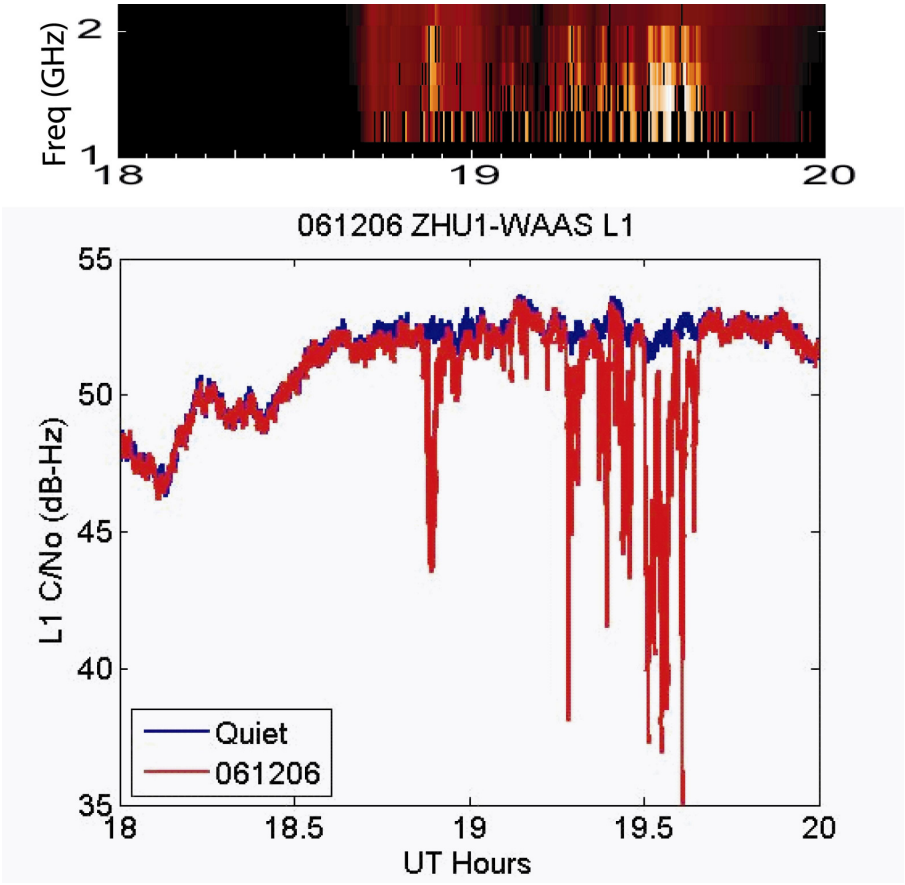

Figure 9. Solar radio burst spectrum (top panel) and GPS receiver response (lower panel).

Within 8 days, two more record-setting solar radio bursts occurred, although the one shown in Figure 9 was the most intense. The fact that this event occurred at solar minimum and was much more intense than any event going back to 1960 is perplexing and makes the prediction of future events difficult. There is some reason to believe that previous operational monitors of solar radio bursts are suspect for intense solar radio bursts and, in fact, those operating during the three events of December 2006 reported much smaller power levels than the research

instruments, of which one example is shown in the top panel of Figure 9. If the operational monitors have been systematically under-reporting the solar radio burst intensities, then the likelihood of power solar radio bursts affecting GPS receivers becomes much more likely during the next solar maximum. There is little we can do except wait and see.

VI. Mitigating Space Weather Effects on GPS Receiver Operation

The first step in mitigating the effects of space weather on GPS signals is to monitor. Scintillations and rapid changes in TEC produced by the ionosphere have unique signatures that can be used to detect their presence. Without monitoring, anomalous receiver performance cannot be properly diagnosed. For example, monitoring is helpful in distinguishing ionospheric scintillations from a flock of birds roosting on or near a receiving antenna.

Second, predict when space weather will occur. There are a variety of aids to help in this effort. NOAA's Space Environment Service is useful for both nowcasting and forecasting magnetic storms and solar flare activity. Satellites located upstream at the L1 Lagrangian point monitoring the solar wind can yield predictions up to an hour in advance. Solar imaging satellites can detect the onset of coronal mass ejections, yielding substantially earlier predictions. These observations are being combined with models to predict the effect on the earth's magnetosphere and ionosphere.

Third, design better GSP receivers. Current receivers are not designed for a scintillating environment, nor is their performance evaluated in the presence of scintillations. They are not able to detect or report if a GPS signal is scintillating. The noise bandwidth of their frequency or phase lock loops is not optimized for a scintillating environment. GPS software receivers may be particularly useful in this application since their operation can be flexible. The receiver tracking loop bandwidth can be increased when the signals are robust and decreased when the signals are scintillating.

Finally, remember that GPS signal scintillations are not the only space weather effect on GPS signals. Solar radio bursts reduce C/No by increasing No, which can threaten GPS receiver operation. Fast-moving ionospheric gradients can produce rapid signal phase changes that also endanger receiver operation.

Suggestions for improving or expanding this introduction may be sent to Prof. Kintner at pmk1@cornell.edu.

Further reading:

Kintner, P.M., B.M. Ledvina, E.R. de Paula, and I.J. Kantor, The size, shape, orientation, speed, and duration of GPS equatorial anomaly scintillations, *Radio Sci., 39*, RS2012, doi:10.1029/2003RS002878, 2004.

Kintner, P.M., and B.M. Ledvina, The ionosphere, radio navigation, and global navigation satellite systems, *Adv. Space Res*., *35*(5), 788-811, 2005.

Cerruti, A.P., P.M. Kintner, S.E. Gary, K.J. Lanzerotti, E. de Paula, and H. Vo, Observed solar radio burst effects on GPS/Wide Area Augmentation System carrier-to-noise ratio, *Space Weather, 4*, S10006, doi:10.1029/2006SW000254, 2006.

Kintner, P. M., B. M. Ledvina, and E. R. de Paula (2007), GPS and ionospheric scintillations, *Space Weather*, *5*, S09003, doi:10.1029/2006SW000260.